Supporting Information for

Efficient Encapsulation of Insulin by Giant Macrocycle as a Powerful Approach to the Inhibition of Its Fibrillation

Ruotong Wang,[a] Zihan Fang,[a] Shenghui Li,[a] Ziliang Zhang,[b] Ming Dong,[a] Junyi Chen,[*a,b] Qingbin Meng[*b] and Chunju Li[*a]

[a] Academy of Interdisciplinary Studies on Intelligent Molecules, Tianjin Key Laboratory of Structure and Performance for Functional Molecules, College of Chemistry, Tianjin Normal University, Tianjin 300387, P. R. China

[b] State Key Laboratory of National Security Specially Needed Medicines, Beijing Institute of Pharmacology and Toxicology, Beijing 100850, P. R. China

[*] Corresponding authors.

Table of Contents

1. General materials and methods

1.1 Materials.

All the reagents and solvents were commercially available and used as received unless other specified purification. Insulin was obtained from Gan & Lee Pharmaceuticals Co., Ltd. (Beijing, China). The 11-*mer* peptide GERGFFYTPKT (P11), 5-*mer* peptide GIVEQ and 6-*mer* peptide FVNQHL were customized from SynPeptide Co., Ltd. Rhodamine 123 (Rho123) was purchased from HEOWNS (Tianjin, China). Histidine was purchased from HEOWNS (Tianjin, China). Phenylalanine was purchased from Energy Chemical (Anhui, China). Arginine and lysine were purchased from Bidepharm (Shanghai, China). Phosphate buffer solution (PBS) was purchased from Yuanye (Tianjin, China). The cell counting kit-8 (CCK-8) was purchased from Dojindo China Co. Ltd. (Shanghai, China). The human normal renal epithelial cells (293T) were purchased from the Cell Resource Center (Beijing, China). The human normal renal epithelial cells (LO2) were purchased from the Cell Resource Center (Beijing, China).

1.2 Instruments.

^{1}H and ^{13}C NMR data were recorded on Bruker Avance III 400 MHz spectrometer. High-resolution mass spectra (HRMS) were determined on Agilent Accurate-Mass Q-TOF 6520 instrument with ESI source and Bruker solariX XR with MALDI source. UV-Vis were received by Agilent Cary 100 UV-Vis. Fluorescence spectroscopic studies were carried out by Agilent Cary 100 fluorescence spectrophotometer. CD experiments were per-formed with a Bio-Logic MOS-450 (Claix, France) at room temperature. The ultrastructure of insulin fibers was observed with a Hitachi TEM, Hitachi H-7650. Cytotoxicity and hemolysis studies were performed on SpectraMax ® M5 plate reader, Molecular Devices. Diabetes was verified using handheld blood glucose meters (OneTouch Verio Flex®)

1.3 Cell and Animal.

293T cells were cultured in DMEM supplemented with 10% FBS, 1% penicillin, and 1% streptomycin. LO2 cells were cultured in 1640 supplemented with 10% FBS,

1% penicillin, and 1% streptomycin. Then cells were incubated at 37 ºC under 5% CO_2 and 90% relative humidity, and passaged every 2 days.

Six-week-old Kunming mice (~20 g body weight) of both sexes were purchased from SPF Biotechnology Co., Ltd. (Beijing, China) for safety evaluation and male C57BL/6J (~20 g body weight) were purchased from Gempharmatech Co., Ltd. (Nanjing, China). All animals maintained at 25 °C in a 12 h light/dark cycle with free access to food and water. Additionally, animals were allowed to acclimate to environment for at least one week before experiments. All experimental procedures were conducted in accordance with the Guide for the Care and Use of Laboratory Animals of the AAALAC, and were approved by the Animal Care and Use Committee of the National Beijing Center for Drug Safety Evaluation and Research (IACUC-2024-002A). Best efforts were made to minimize the number of animals used and their suffering.

1.4 Fluorescence titration.

To quantitatively assess the binding constant of insulin/PP[3]AS, fluorescence competitive titration was performed at 298 K in a 10 mM PBS of pH 7.4 and Rho123 was chosen as an optical indicator. The experimental details were followed as the procedure reported previously.[1-3]

1.5 Molecular geometry calculation.

Geometry optimization and final heat analysis of insulin/PP[3]AS complex were performed using the PM7 method. All calculations were carried out with MOPAC.[4-6]

1.6 UV-Vis absorbance assay.

The UV-Vis absorbance assay was received by Agilent Cary 100 UV-Vis. First, 12mg of insulin was dissolved in 200μL of a combined solution of 25 mmol/L HCl and 100 mmol/L NaCl (pH ~ 1.7) and then diluted into PBS (10 mmol/L, pH 7.4). For inhibition experiments, the insulin solutions (172.0 μmol/L) were incubated at 65 °C in the absence or presence of PP[3]AS. For disaggregation experiments, the insulin solution (172.0 μmol/L) was incubated alone at 65 °C. At the time point of 72 h and 144h, PP[3]AS (344.0 μmol/L in PBS) was added, and the pure PBS solution was added

into another sample as a control. Absorbance values at 540 nm of different solutions were measured at different time points. The experiment was repeated three times independently.

1.7 Circular dichroism measurements.

CD experiments were per-formed with a Bio-Logic MOS-450 (Claix, France) at room temperature. The experimental conditions were as follows: speed of 50 $nm \cdot min^{-1}$, time response of 2 s, resolution of 0.5 nm, bandwidth of 4.0 nm, and cell path length of 1.0 mm. All spectra were converted to a uniform scale after subtraction of the background. The recorded curves were smoothed with standard parameters.

1.8 Transmission electron microscopy.

The TEM samples were characterized by a Hitachi TEM (Hitachi H-7650, Japan) at an accelerating voltage of 80 kV. 10 μL of each sample was placed on the carbon-coated copper grids with a pipette for 10 min. Then the excess solution was removed by filter paper. Subsequently, the samples were negatively stained with 2% tungstophosphoric acid for 3 min and the excess liquid was drained. In the end, the samples were transferred to a desiccator to dry overnight.

1.9 *In vitro* cytotoxicity studies.

The relative cytotoxicity of PP[3]AS against 293T and LO2 cells was assessed *in vitro* using CCK-8 according to the manufacturer's instructions. Cells were seeded into 96-well plates at a density of 8000 cells/well with 100 μL culture medium. After 24 h incubation, the culture medium was replaced with 100 μL of a fresh medium containing various concentrations of PP[3]AS, 5 holes were arranged in parallel for each concentration group, and set a control group. The cells were incubated for another 24 h. CCK-8 solution was added to each well, followed by incubation at 37 °C for 0.5 h. Subsequently, the plates were measured at 450 nm using a microplate reader. All experiments were carried out five independent times.[7,8]

1.10 Safety evaluations of PP[3]AS.

As a preliminary study on the safety profile of PP[3]AS, twelve Kunming mice (~20 g) were randomly divided into two groups (n=6 in each group). PP[3]AS was

subcutaneously injected at a total dose of 1 $mg \cdot kg^{-1}$. In the control group, mice were administrated with PBS. The body weight of the mice was monitored every day at a defined time point and their general behaviors were observed. After 18 days, the mice were euthanized. Blood samples were collected for hematological analysis and major organs were isolated for calculation of organ index and histopathological analyses.

1.11 *In vivo* insulin performance.

A chemically induced diabetes mouse model was established in male C57BL/6J mice using streptozotocin (STZ), according to common protocols.[9] Mice were fasted for 4 h prior to injection with STZ at 100 mg/kg i.p., dissolved in pH 4.5 citrate buffer. Treated mice were fasted for an additional 0.5 h and were then supplied with food and water as normal. Treated mice were allowed to develop diabetes for 7 days, and diabetes was verified using handheld blood glucose meters (OneTouch Verio Flex®), targeting unfasted blood glucose levels above 16.7 mM. STZ-induced diabetic mice were fasted for 6 h before assessing insulin performance. Mice were bled at the beginning of the study, and any mouse with a fasting blood glucose level below 11.1 mM was triaged from the study. Mice were then randomized and injected subcutaneously with insulin dosed at 100 $\mu g \cdot kg^{-1}$ either alone or formulated with 1 molar equivalent of PP[3]AS. Blood glucose readings were collected at predetermined intervals using a handheld glucose meter for 300 min following insulin injection.

2 Synthesis of PP[3]AS

2.1 Synthesis of PP-OMe.

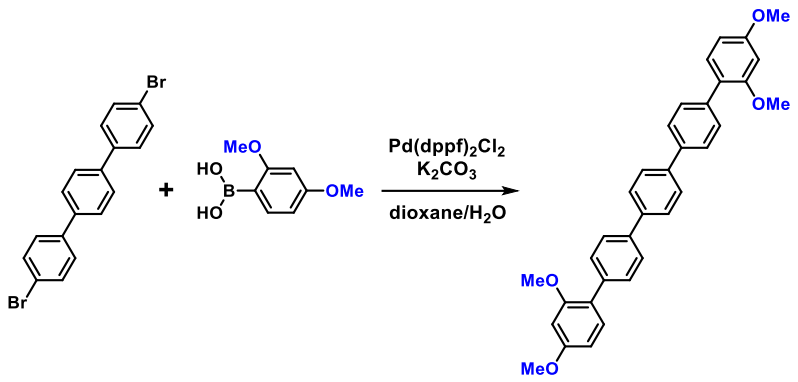

PP-OMe

To a 500 mL flask were added 4,4''-dibromo-terphenyl (5.05g, 13.1 mmol), 2,4-Dimethoxyphenylboronic acid (5.92 g, 32.5 mmol), dichloro[1,1'-bis(diphenylphosphino)ferrocene]palladium (0.479g, 0.654 mmol), potassium carbonate (7.19 g, 52.0 mmol), 1,4-dioxane (200 mL) and water (40.0 mL). The mixture was stirred and refluxed under nitrogen atmosphere for 12 hours. After cooling down to room temperature, most of the solvents were removed under reduced pressure, then extracted with dichloromethane. The organic layer was dried over anhydrous sodium sulfate and subsequently concentrated under reduced pressure. The residue was purified by column chromatography on silica gel to afford PP-OMe as a white solid (4.20g, 64.0 %). ^{1}H NMR (400 MHz, $CDCl_3$) δ (ppm): 7.72 (s, 4H), 7.68 (d, J = 8.4 Hz, 4H), 7.61 (d, J = 8.4 Hz, 4H), 7.31 (d, J = 8.8 Hz, 2H), 6.61 (d, J = 2.4 Hz,1H), 6.59 (s, 3H), 3.87 (s, 6H), 3.84 (s, 6H). ^{13}C NMR (101 MHz, $CDCl_3$) δ (ppm): 159.4, 156.6, 138.8, 137.8, 136.5, 130.9, 130.2, 128.8, 127.6, 126.5, 126.4, 126.3, 125.6, 122.2, 103.8, 98.1, 54.6, 54.4, 52.4, 28.7, 13.1. HRMS (ESI) m/z: $[M+Na]^+$ calcd. for $C_{34}H_{30}O_4Na^+$ 525.2042; found, 525.2036.

2.2 Synthesis of PP[3]A-OMe.

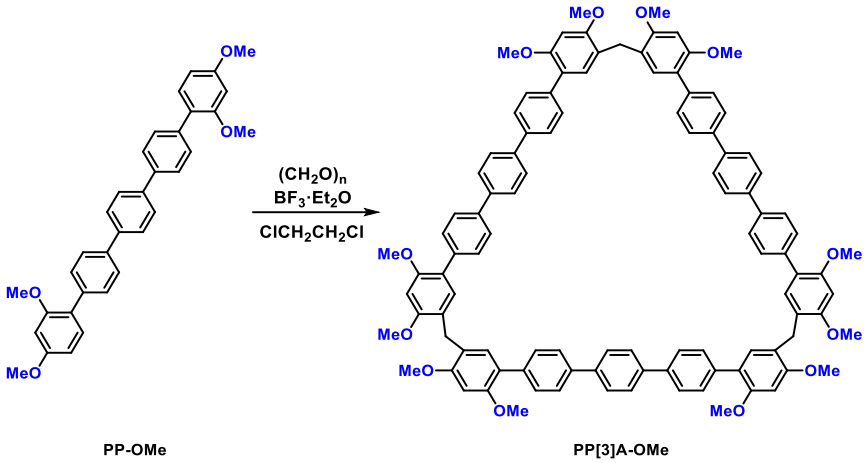

To the solution of PP-OMe (300 mg, 0.597 mmol) and paraformaldehyde (44.80 mg, 1.49 mmol) in 1,2-dichloroethane (15 mL) was added boron trifluoride etherate (30.0 μL, 0.239 mmol) and stirred at room temperature for 10 minutes. After quenching with a saturated sodium bicarbonate solution, the water phase was extracted with dichloromethane and the organic phase was washed with saturated sodium chloride solution, respectively. The organic phase was then dried over anhydrous sodium sulfate and subsequently concentrated under reduced pressure. The residue was purified by column chromatography on silica gel to afford PP[3]A-OMe as a white solid (398 mg, 43.2 %). ^{1}H NMR (400 MHz, CDCl3) δ (ppm): 7.69 (s, 12H), 7.65 (d, J = 8.3 Hz, 12H), 7.57 (d, J = 8.3 Hz, 12H), 7.04 (s, 6H), 6.61 (s, 6H), 3.98 (s, 6H), 3.91 (s, 18H), 3.87 (s, 18H). ^{13}C NMR (101 MHz, $CDCl_3$) δ (ppm): 157.9, 155.9, 139.8, 138.6, 137.7, 131.9, 129.9, 127.3, 126.6, 122.1, 121.6, 96.2, 56.0, 55.9, 27.8. MALDI-TOF MS: calcd. for $C_{105}H_{90}O_{12}$ 1542.6432; found, 1542.6427.

2.3 Synthesis of PP[3]A-OH.

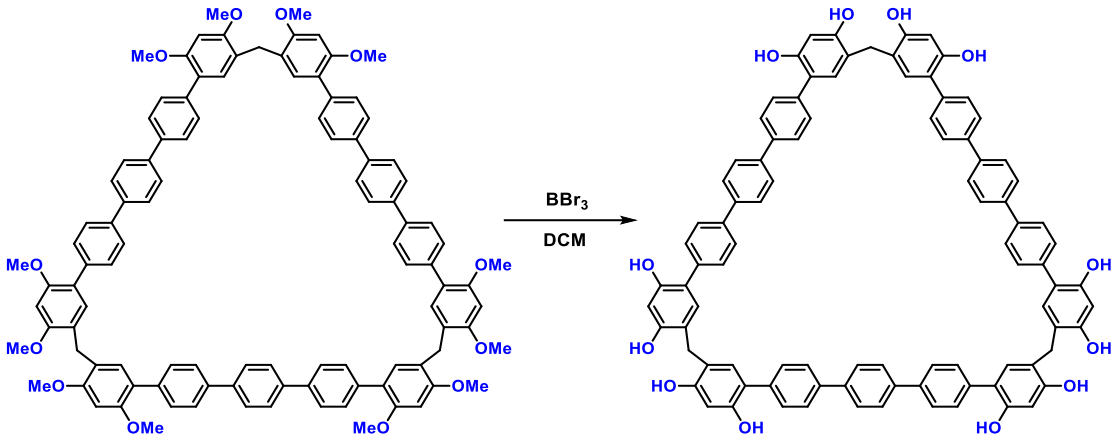

To a solution of PP[3]A-OMe (100 mg, 0.0648 mmol) in 150 mL dichloromethane and replace argon three times. Put the flask in an ice bath and dropwise boron tribromide (0.740 mL, 7.83 mmol) into the reaction solution slowly. The resulting mixture was stirred at room temperature for 3 days. Add ice water to quench the reaction. The product was extracted with ethyl acetate three times. Combine the organic phase, and dried to afford a brownness solid (85.24 mg, 95.7 % yield). The product PP[3]A-OH proceeded directly to the next reaction. H NMR (400 MHz, $(CD_3)_2CO$) δ (ppm): 7.78 (s, 12H), 7.70 (d, J = 8.3 Hz, 12H), 7.66 (d, J = 8.4 Hz, 12H), 7.27 (s, 6H), 6.61 (s, 6H), 3.94 (s, 6H). ^{13}C NMR (101 MHz, $(CD_3)_2CO$) δ (ppm): 155.3, 154.3, 154.1, 140.5, 139.1, 138.8, 132.8, 130.5, 128.0, 127.1, 121.1, 120.5, 104.2. HRMS (ESI) m/z: $[M-2H]^{2-}$ calcd. for $C_{93}H_{64}O_{12}^{2-}$ 686.2204; found, 686.2204.

2.4 Synthesis of PP[3]AS.

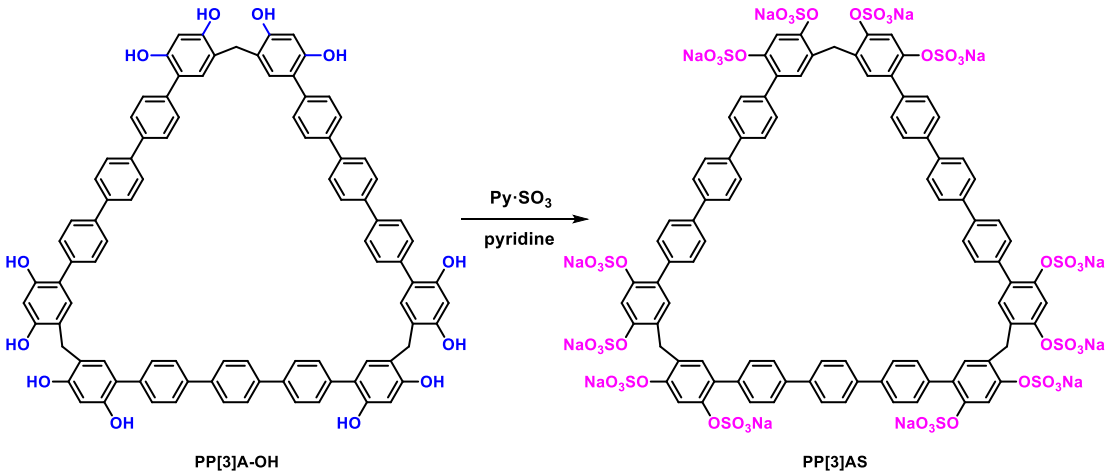

To a mixture of PP[3]A-OH (100 mg, 0.0728 mmol) and pyridine sulfur trioxide complex (716 mg, 4.50 mmol) was added dry pyridine (10.0 mL). The resulting mixture was stirred at 75 °C under an argon atmosphere for 12 hours. The reaction mixture was allowed to cool to room temperature and pyridine poured out. The crude solid was washed with dichloromethane and ethyl acetate for two times. Then, adjusted to pH = 7.5 by slow addition of saturated aqueous sodium bicarbonate solution. After the addition of ethanol (30.0 mL), the crude product was collected by centrifugation at 3500 rpm × 10 min. The precipitate was suspended in ethanol (30.0 mL × 2), sonicated for 3 minutes, and solid collected by centrifugation. The crude solid was redissolved in methanol. Desalination by centrifugation. After drying under a high vacuum, PP[3]AS was obtained as a light yellow solid (131 mg, 69.3 % yield). ^{1}H NMR (400 MHz, $(CD_3)_2SO$) δ (ppm): 7.76 (s, 20H), 7.65 (d, *J* = 6.9 Hz, 12H), 7.58 (d, *J* = 6.0 Hz, 12H), 6.84 (s, 4H), 4.10 (s, 6H). ^{13}C NMR (101 MHz, $(CD_3)_2SO$) δ (ppm): 138.8, 137.5, 137.5, 129.7, 127.8, 127.0, 125.9, 111.9, 99.5. HRMS (ESI): $[M-6Na]^{6-}$ calcd. for $C_{93}H_{54}O_{48}S_{12}Na_6^{6-}$ 410.1311; found, 410.1314.

3 Supporting results and experimental raw data

3.1 Characterization of synthetic molecular host.

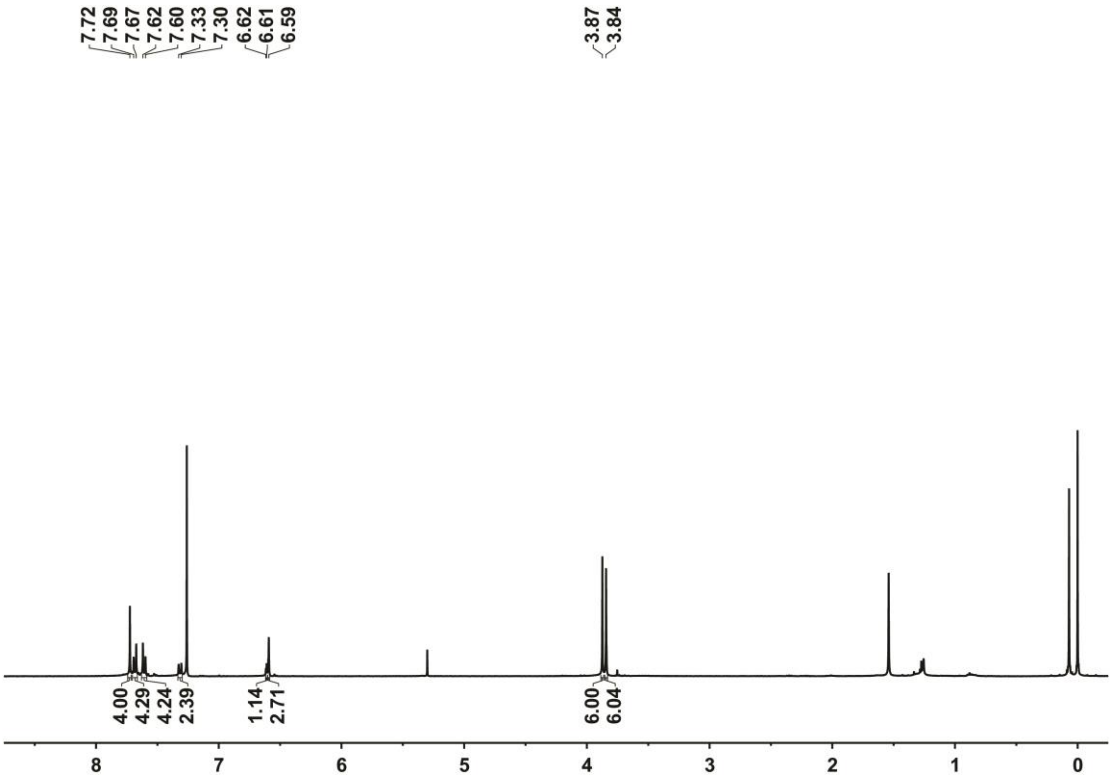

Fig. S1 ^{1}H NMR spectrum (400 MHz, $CDCl_3$) of PP-OMe.

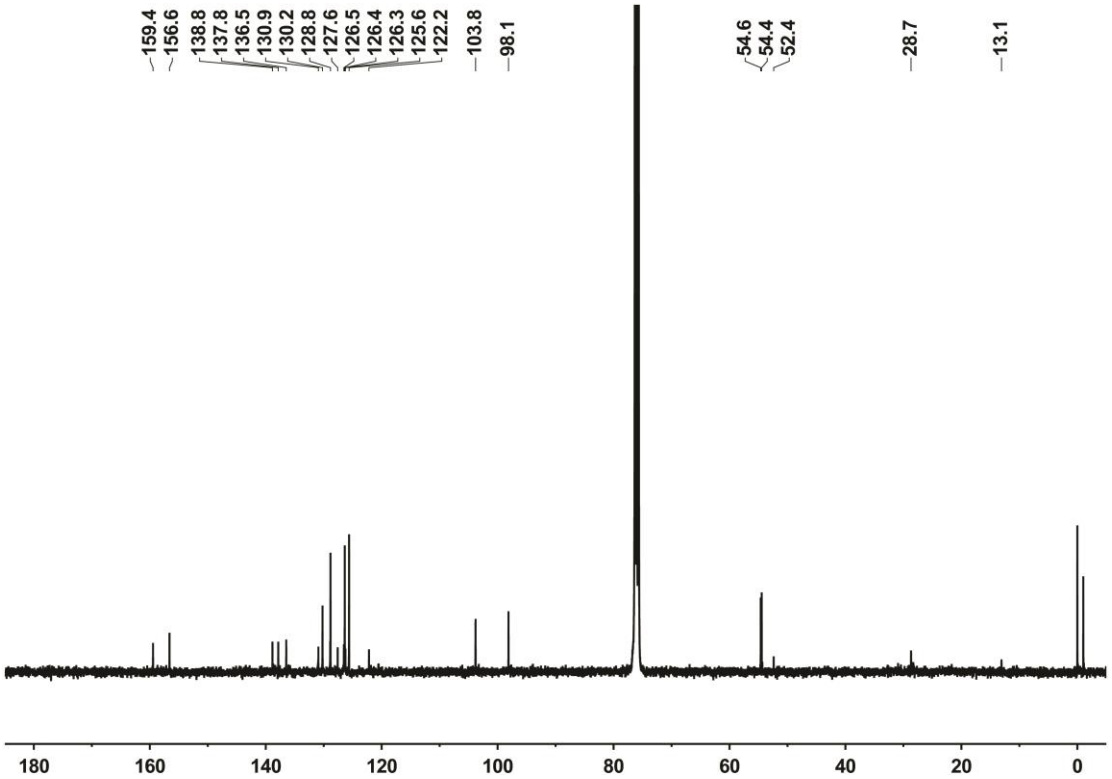

Fig S2 ^{13}C NMR spectrum (101 MHz, $CDCl_3$) of PP-OMe.

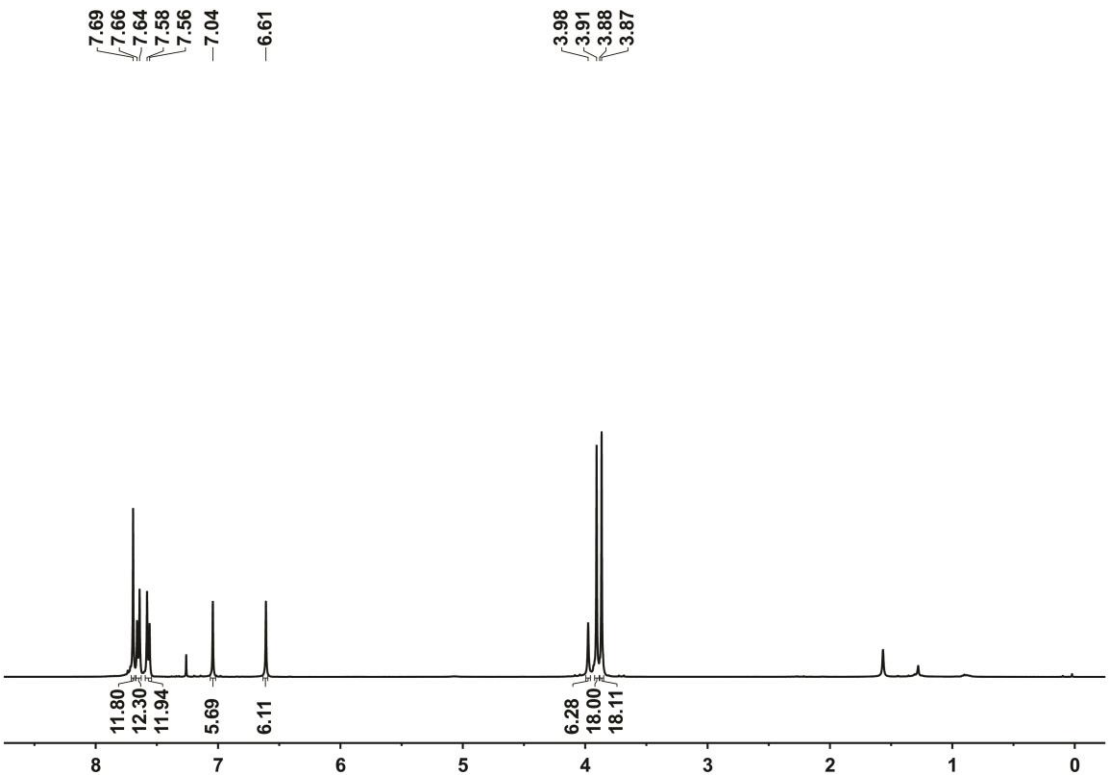

Fig. S3 ^{1}H NMR spectrum (400 MHz, $CDCl_3$) of PP[3]A-OMe.

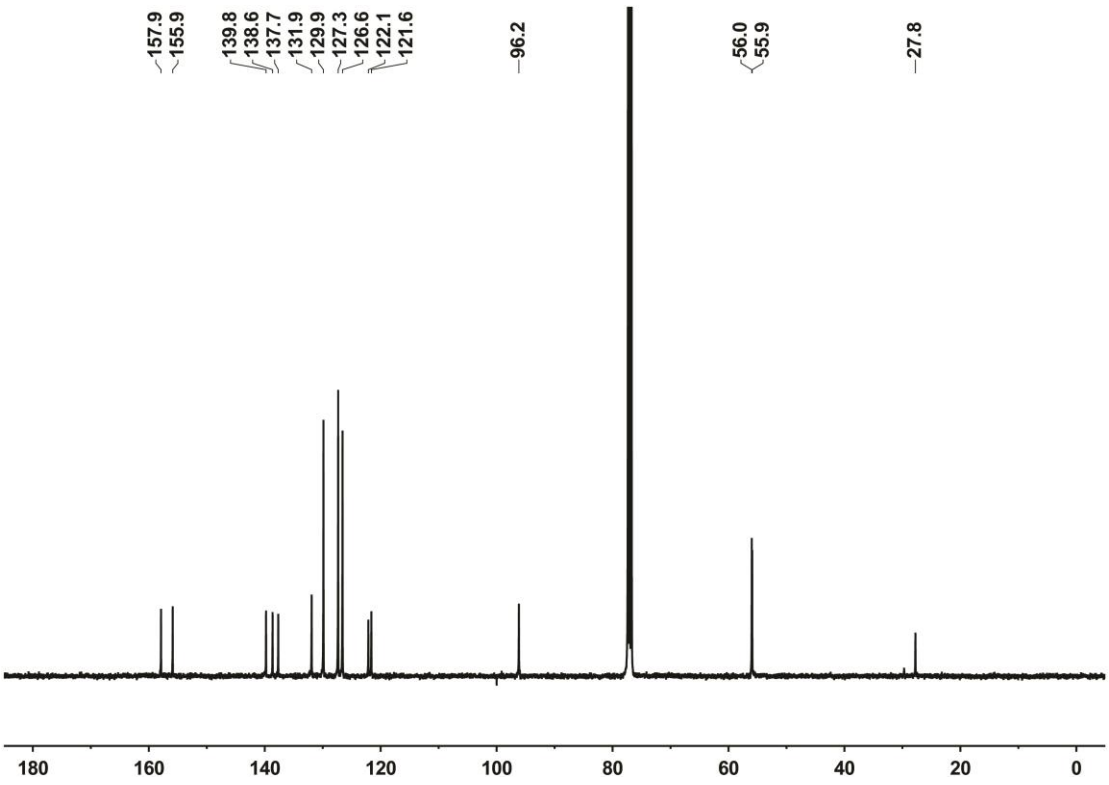

Fig. S4 ^{13}C NMR spectrum (101 MHz, $CDCl_3$) of PP[3]A-OMe.

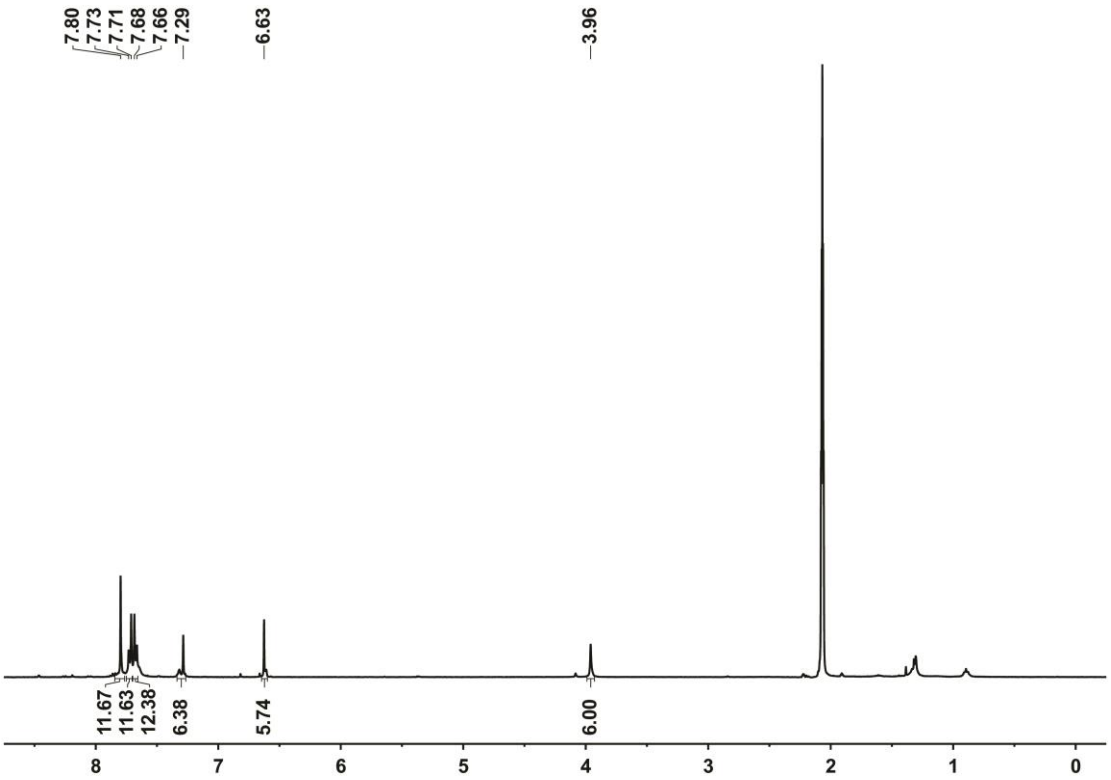

Fig. S5 ^{1}H NMR spectrum (400 MHz, $(CD_3)_2CO$) of PP[3]A-OH.

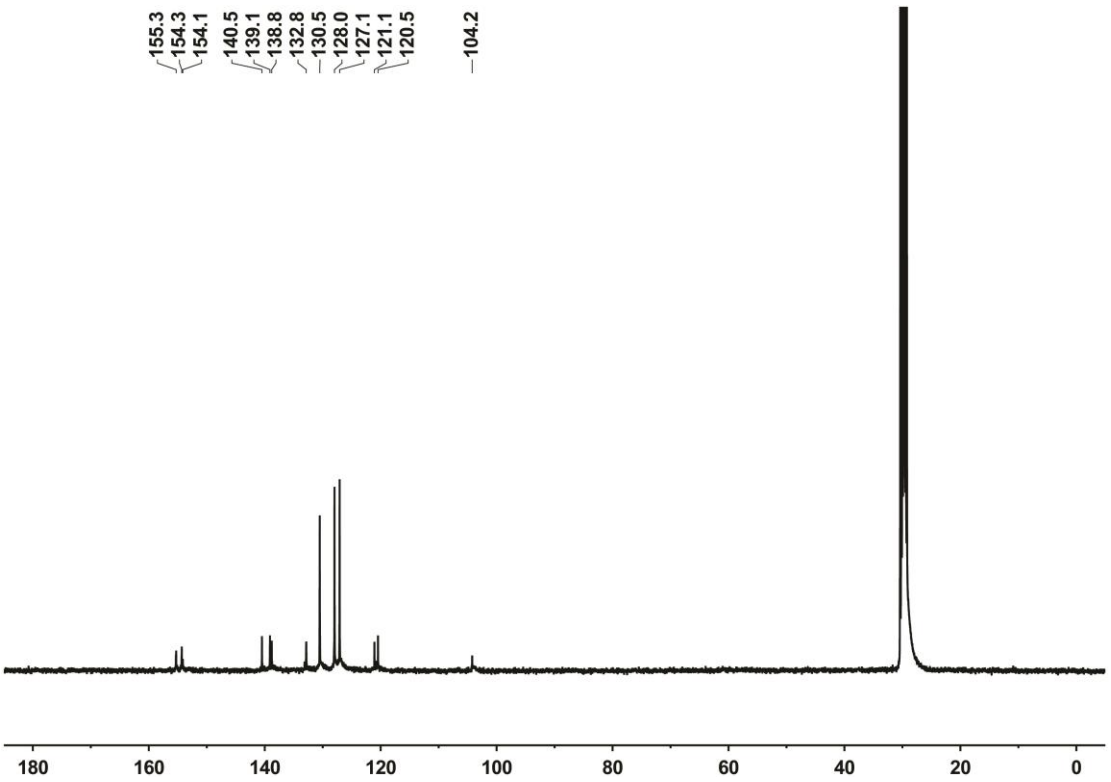

Fig. S6 ^{13}C NMR spectrum (101 MHz, $(CD_3)_2CO$) of PP[3]A-OH.

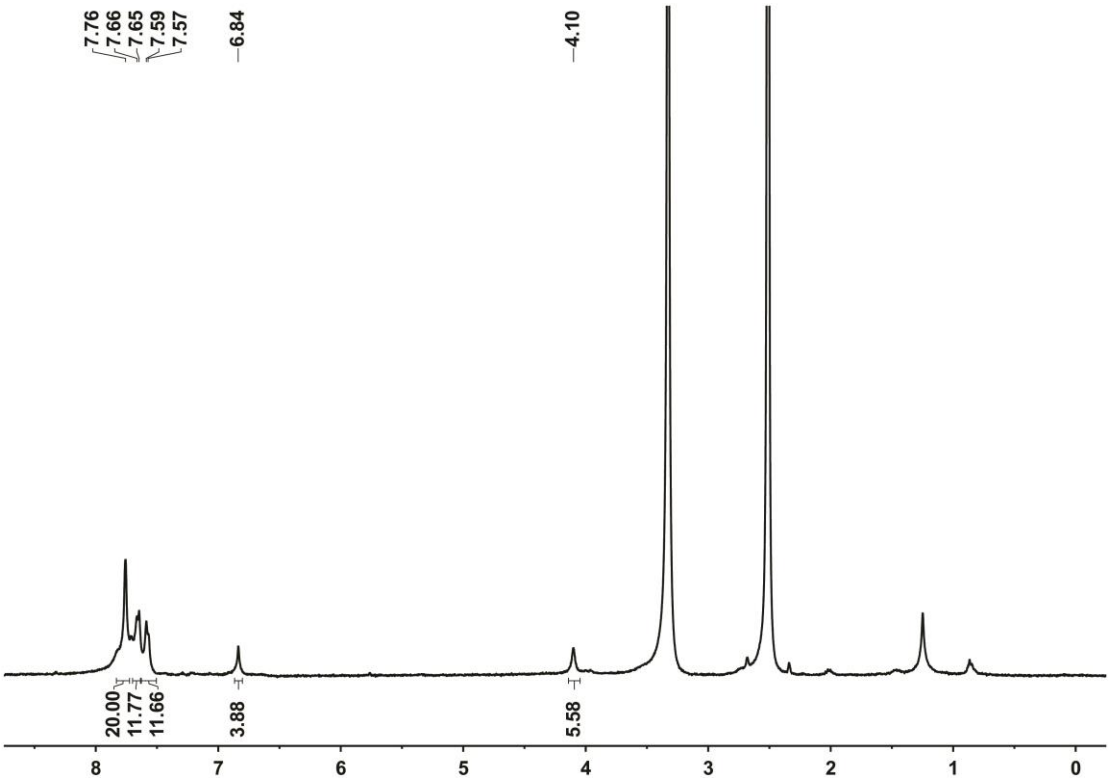

Fig. S7 ^{1}H NMR spectrum (400 MHz, $(CD_3)_2SO$) of PP[3]AS.

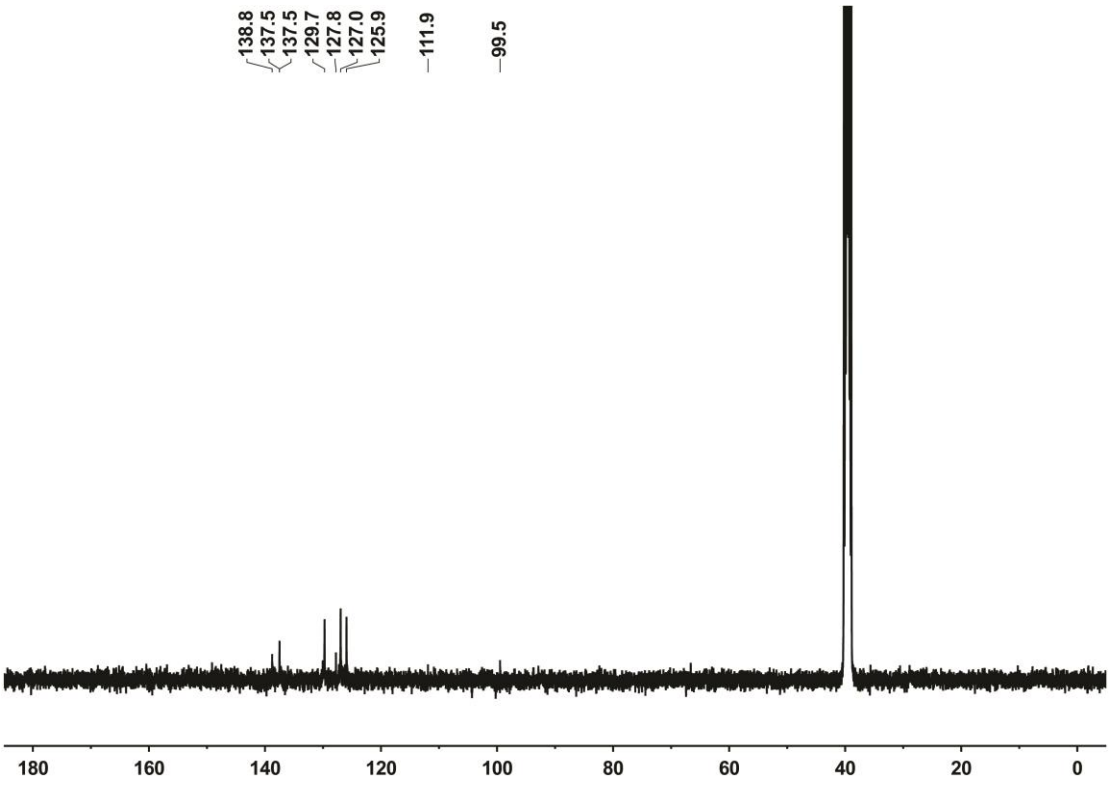

Fig. S8 ^{13}C NMR spectrum (101 MHz, $(CD_3)_2SO$) of PP[3]AS.

3.2 Job's plot analysis for complexation of Rho123 with PP[3]AS

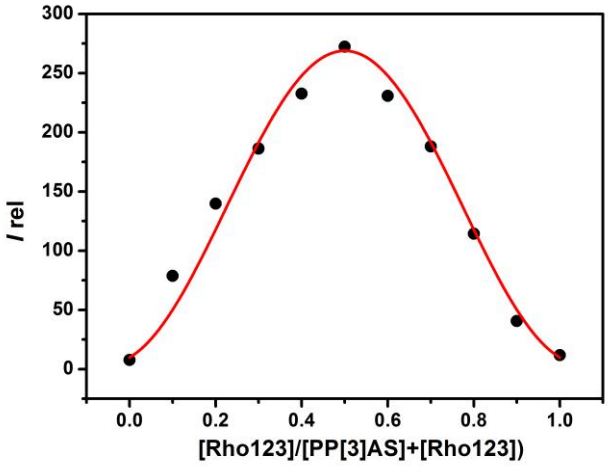

Fig. S9 Job's plot for PP[3]AS with Rho123 in 10 mM PBS buffer at pH 7.4 (λ_{ex} = 500 nm, λ_{em} = 525 nm, [PP[3]AS] + [Rho123] = 1.0 μM).

3.3 Direct fluorescence titration of Rho123/PP[3]AS.

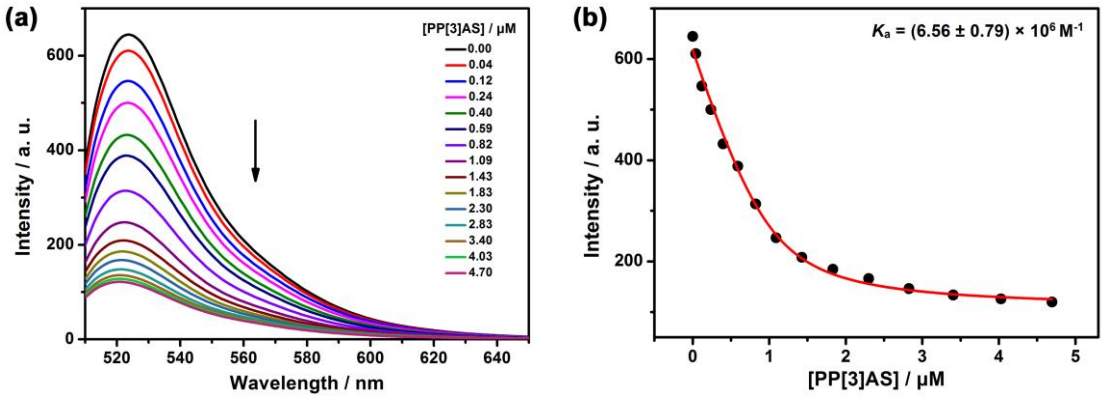

Fig. S10 (a) Direct fluorescence titration of Rho123 (1.00 μM) with PP[3]AS in 10 mM PBS buffer at pH 7.4, λ_{ex} = 500 nm. (b) The associated titration curve at λ_{em} = 525 nm and fit according to a 1:1 binding stoichiometry.

3.4 Optimized geometries of PP[3]AS, insulin and insulin/PP[3]AS.

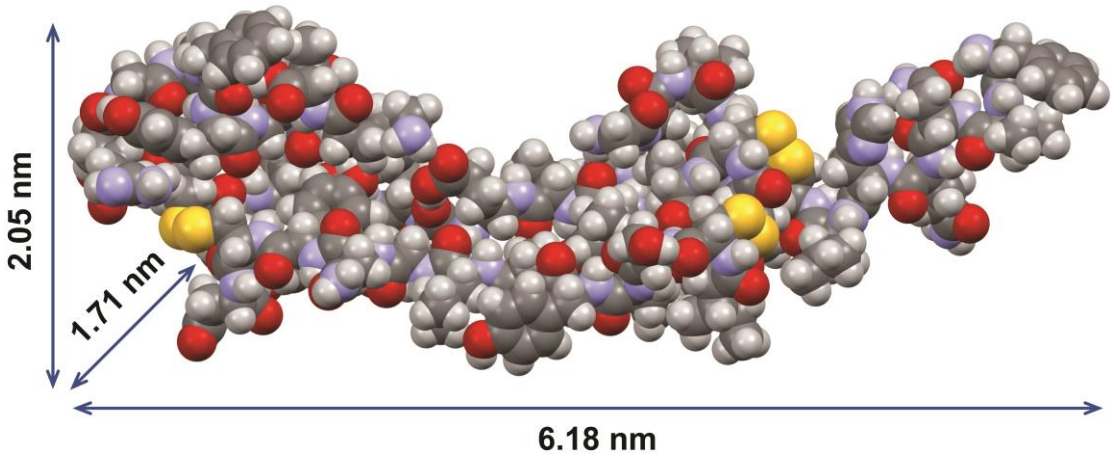

Fig. S11 The optimized molecular structure of insulin in water (MOPAC with the PM7 method).

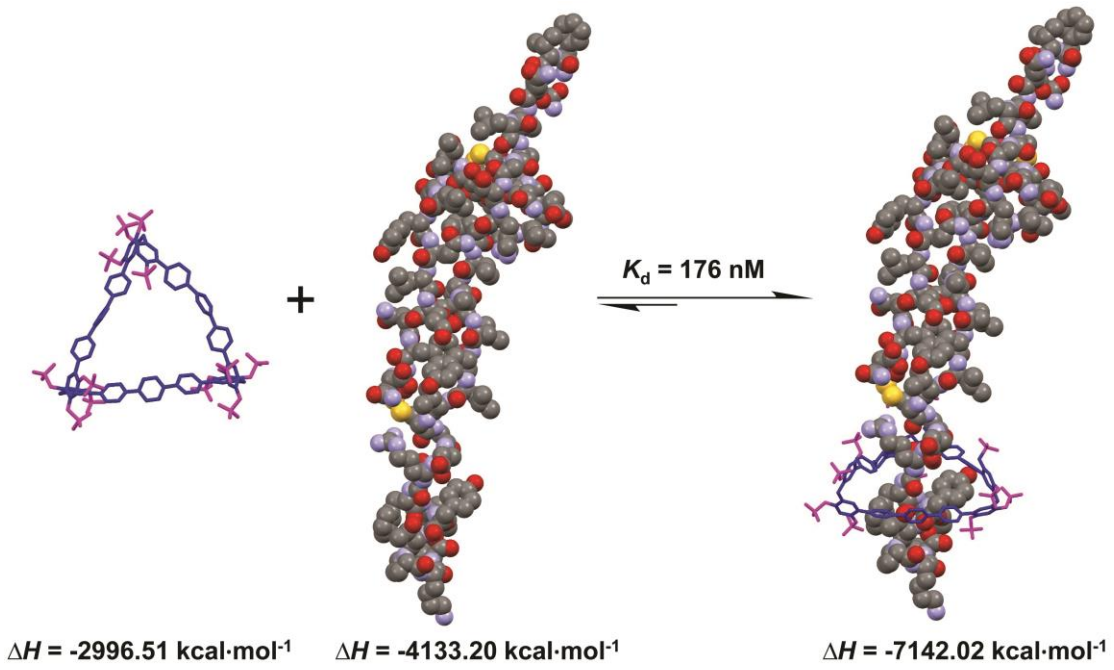

Fig. S12 Optimized binding mode and final heat of PP[3]AS, insulin and insulin/PP[3]AS in water (MOPAC with the PM7 method).

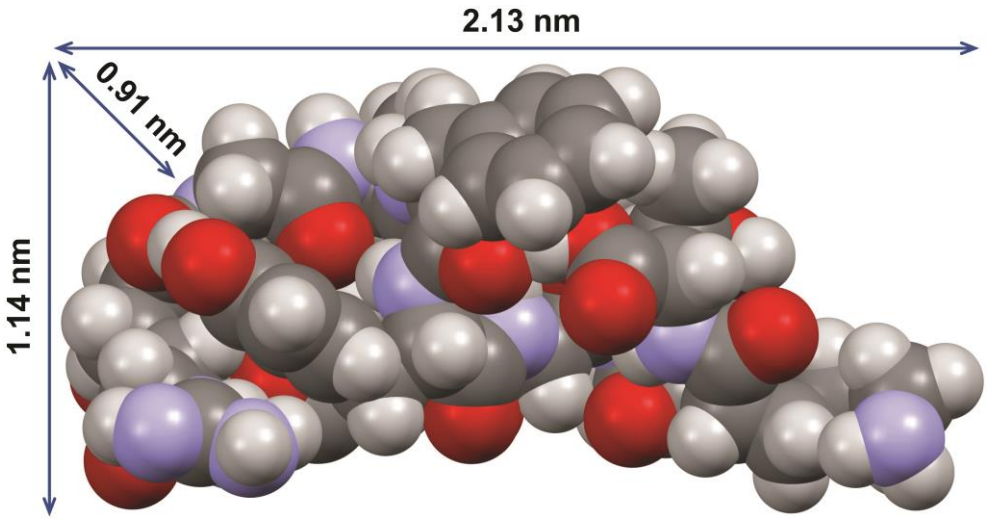

Fig. S13 Enlarged molecular structure of C-terminal 11-mer peptide sequence of B chain in water (MOPAC with the PM7 method).

3.5 Competitive titration of three control compounds.

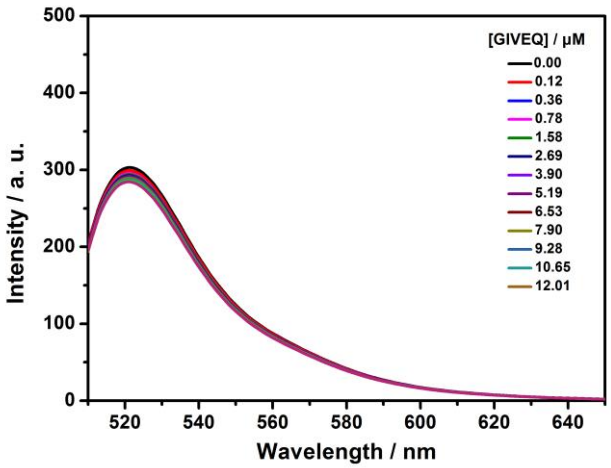

Fig. S14 Competitive fluorescence titration of N-terminal 5-mer peptide sequence of A chain in the presence of Rho123 (0.50 μM)/PP[3]AS (0.50 μM) in 10 mM PBS buffer at pH 7.4, λ_{ex} = 500 nm. The recovery of fluorescence is too small relative to the range of quenching, so no reasonable association constant can be obtained.

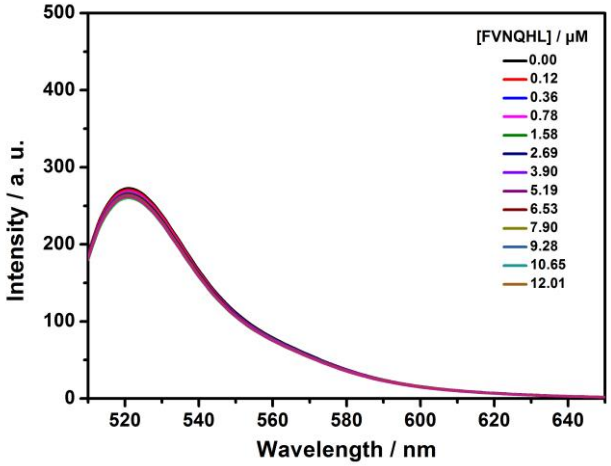

Fig. S15 Competitive fluorescence titration of N-terminal 6-mer peptide sequence of B chain in the presence of Rho123 (0.50 μM)/PP[3]AS (0.50 μM) in 10 mM PBS buffer at pH 7.4, λ_{ex} = 500 nm. The recovery of fluorescence is too small relative to the range of quenching, so no reasonable association constant can be obtained.

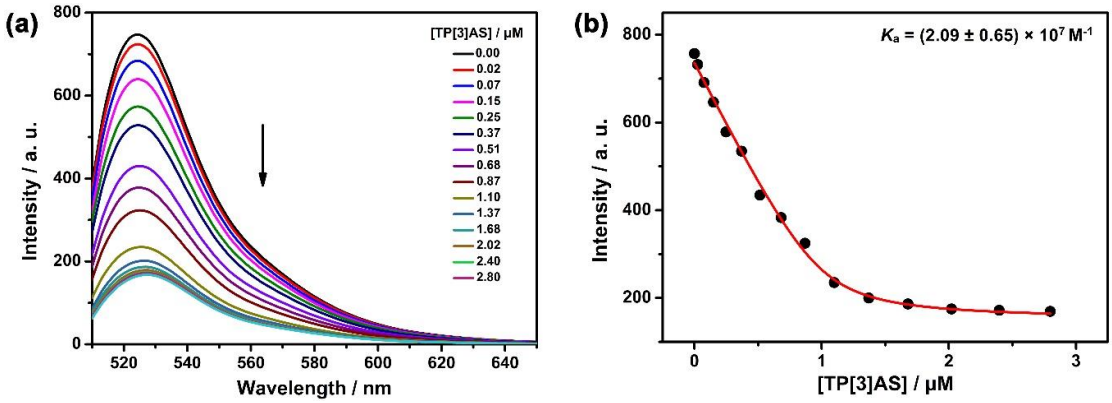

Fig. S16 (a) Direct fluorescence titration of Rho123 (1.00 μM) with TP[3]AS in 10 mM PBS buffer at pH 7.4, λ_{ex} = 500 nm. (b) The associated titration curve at λ_{em} = 525 nm and fit according to a 1:1 binding stoichiometry.

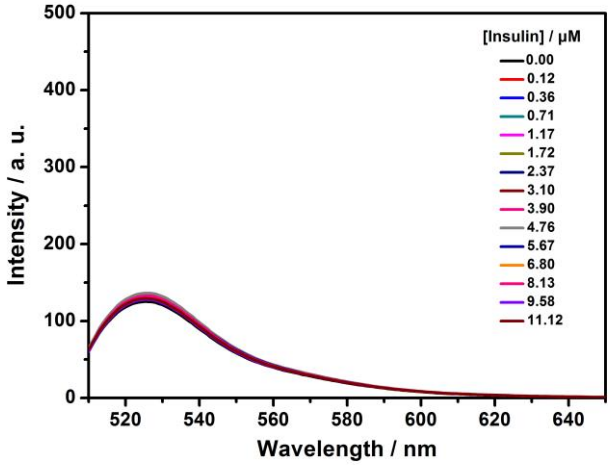

Fig. S17 Competitive fluorescence titration of insulin in the presence of Rho123 (1.00 μM)/TP[3]AS (1.00 μM) in 10 mM PBS buffer at pH 7.4, λ_{ex} = 500 nm. The recovery of fluorescence is too small relative to the range of quenching, so no reasonable association constant can be obtained.

3.6 Binding of PP[3]AS with lysine, arginine, phenylalanine, tyrosine and proline.

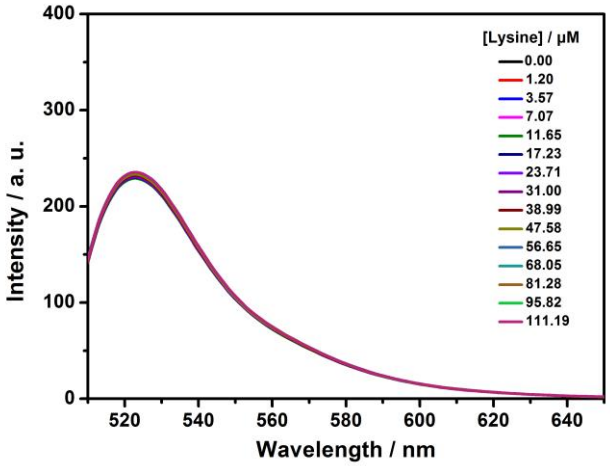

Fig. S18 Competitive fluorescence titration of lysine in the presence of Rho123 (0.50 μM)/PP[3]AS (0.50 μM) in 10 mM PBS buffer at pH 7.4, λ_{ex} = 500 nm. The recovery of fluorescence is too small relative to the range of quenching, so no reasonable association constant can be obtained.

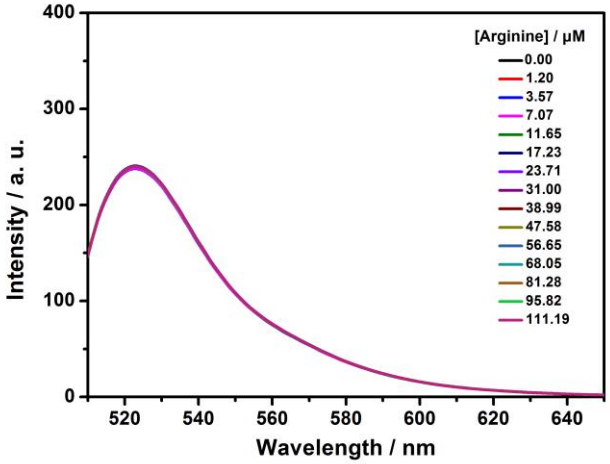

Fig. S19 Competitive fluorescence titration of arginine in the presence of Rho123 (0.50 μM)/PP[3]AS (0.50 μM) in 10 mM PBS buffer at pH 7.4, λ_{ex} = 500 nm. The recovery of fluorescence is too small relative to the range of quenching, so no reasonable association constant can be obtained.

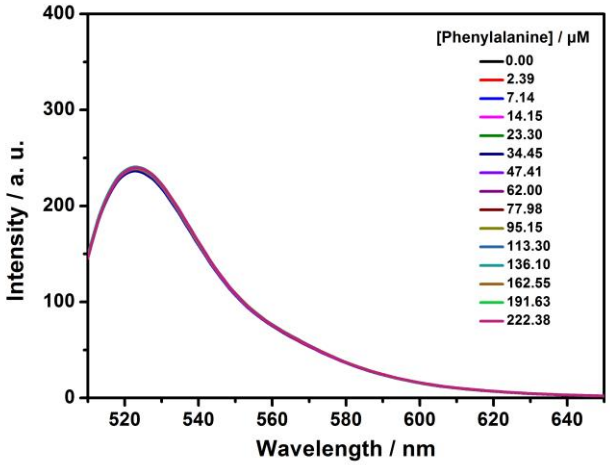

Fig. S20 Competitive fluorescence titration of phenylalanine in the presence of Rho123 (0.50 μM)/PP[3]AS (0.50 μM) in 10 mM PBS buffer at pH 7.4, λ_{ex} = 500 nm. The recovery of fluorescence is too small relative to the range of quenching, so no reasonable association constant can be obtained.

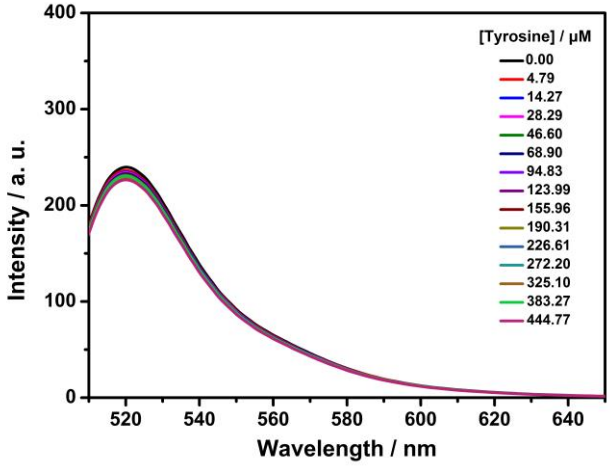

Fig. S21 Competitive fluorescence titration of tyrosine in the presence of Rho123 (0.50 μM)/PP[3]AS (0.50 μM) in 10 mM PBS buffer at pH 7.4, λ_{ex} = 500 nm. The recovery of fluorescence is too small relative to the range of quenching, so no reasonable association constant can be obtained.

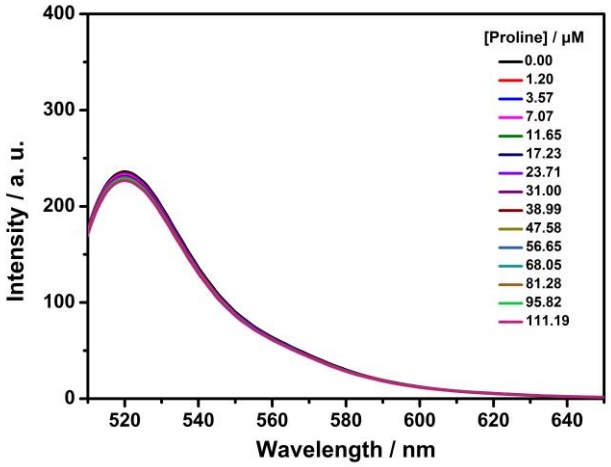

Fig. S22 Competitive fluorescence titration of proline in the presence of Rho123 (0.50 μM)/PP[3]AS (0.50 μM) in 10 mM PBS buffer at pH 7.4, λ_{ex} = 500 nm. The recovery of fluorescence is too small relative to the range of quenching, so no reasonable association constant can be obtained.

3.7 The fluorescence responses toward biologically important species.

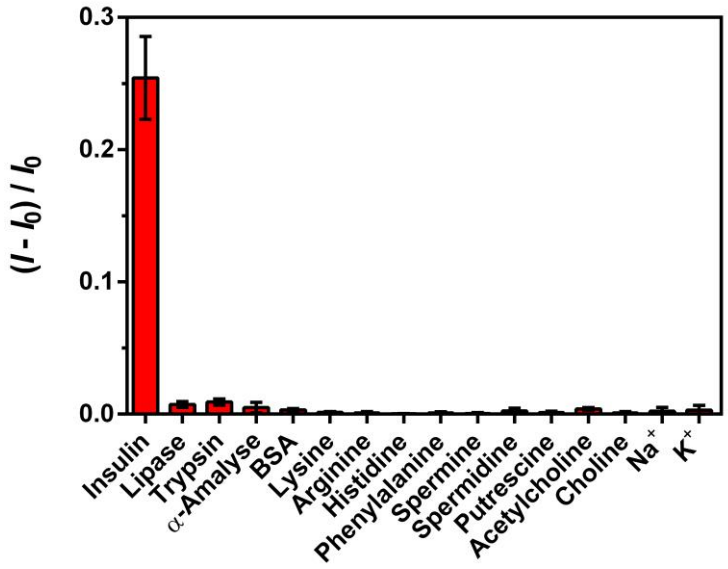

Fig. S23 Fluorescence responses of Rho123 (0.50 μM)/PP[3]AS (0.50 μM) at 525 nm (λ_{ex} = 500 nm) upon addition of Insulin and various biological co-existing species (10 μM) in PBS buffer. Data were from n = 3 independent experiments and are presented as mean ± S.D.

3.8 Influence of insulin aggregation by two control macrocycles.

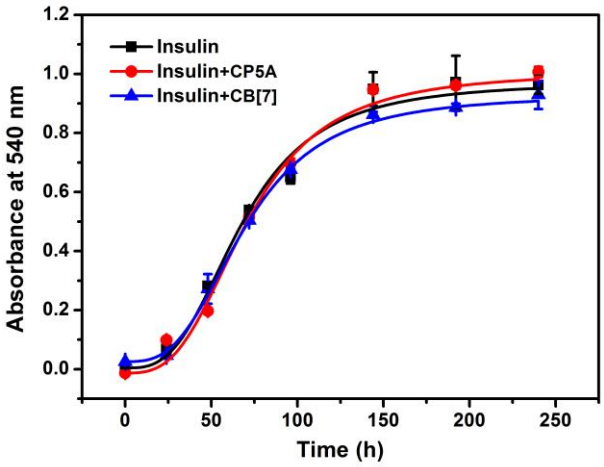

Fig. S24 Kinetics of insulin (172 μM) aggregation in 10 mM PBS buffer at pH 7.4, monitored by absorbance assay in the absence and presence of CP5A (172 μM) and CB[7]. Data are from n = 3 independent experiments and presented as mean ± SD.

3.9 *In vitro* cytotoxicity assay of PP[3]AS.

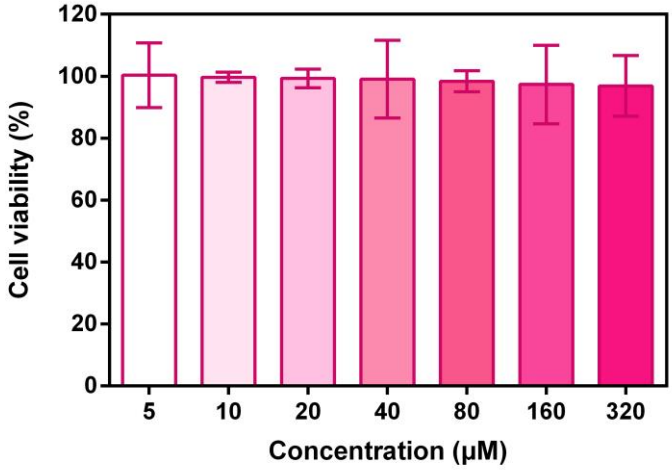

Fig. S25 Relative cell viability of LO2 cells treated with different concentrations of PP[3]AS for 24 h (mean ± S.D., n = 5).

3.10 Blood routine and blood biochemical examination of PP[3]AS.

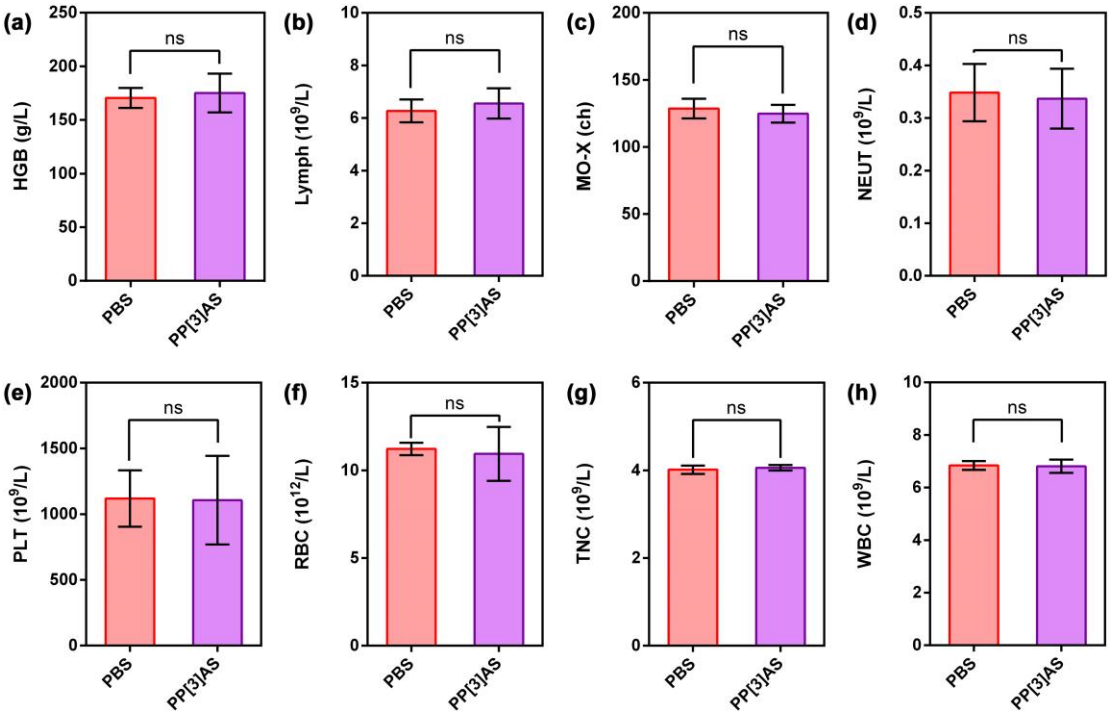

Fig. S26 (a) hemoglobin (HGB), (b) lymphocytes (Lymph), (c) monocytes-X (MO-X), (d) neutrophils (NEUT), (e) platelet (PLT), (f) red blood cell (RBC), (g) troponin-C (TNC) and (h) white blood cell (WBC) levels from mice administered with PBS and PP[3]AS. Data presented are the mean ± S.D. (n = 3). ns represents "no significant difference" between the experimental group and the control group.

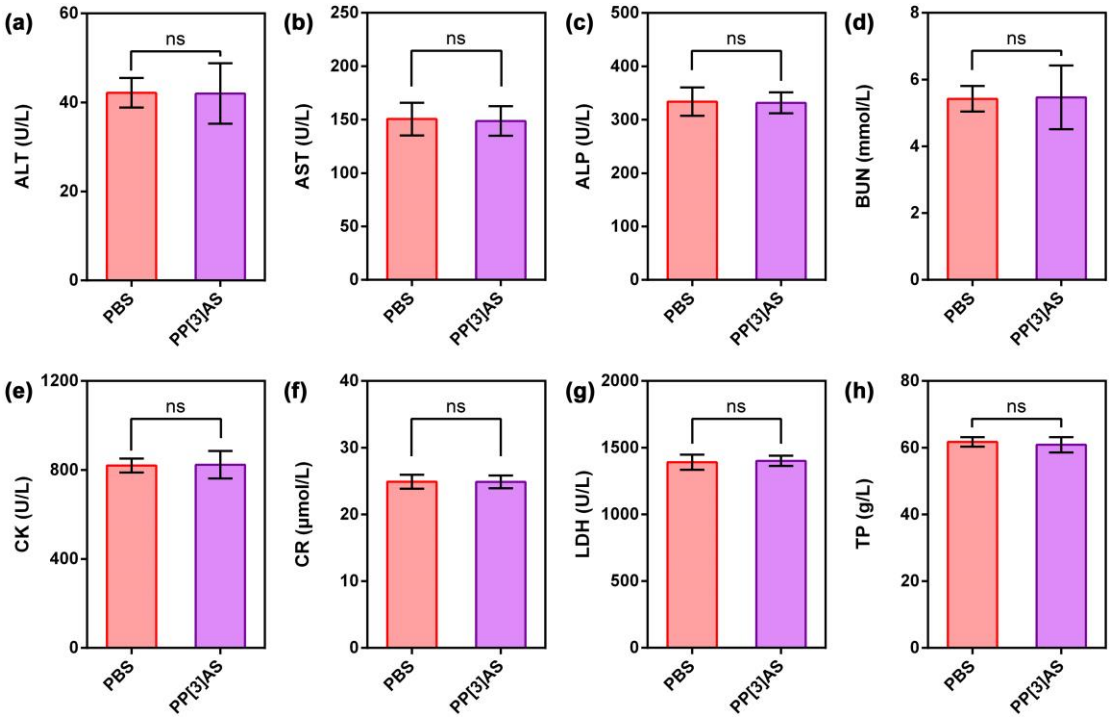

Fig. S27 (a) alanine transaminase (ALT), (b) aspartic transaminase (AST), (c) alkaline phosphatase (ALP), (d) blood urea nitrogen (BUN), (e) creatine kinase (CK), (f) creatinine (CREA), (g) lactate dehydrogenase (LDH) and (h) total protein (TP) levels from mice administered with PBS and PP[3]AS. Data presented are the mean ± S.D. (n = 3). ns represents "no significant difference" between the experimental group and the control group.

3.11 Histopathological examination of major organs.

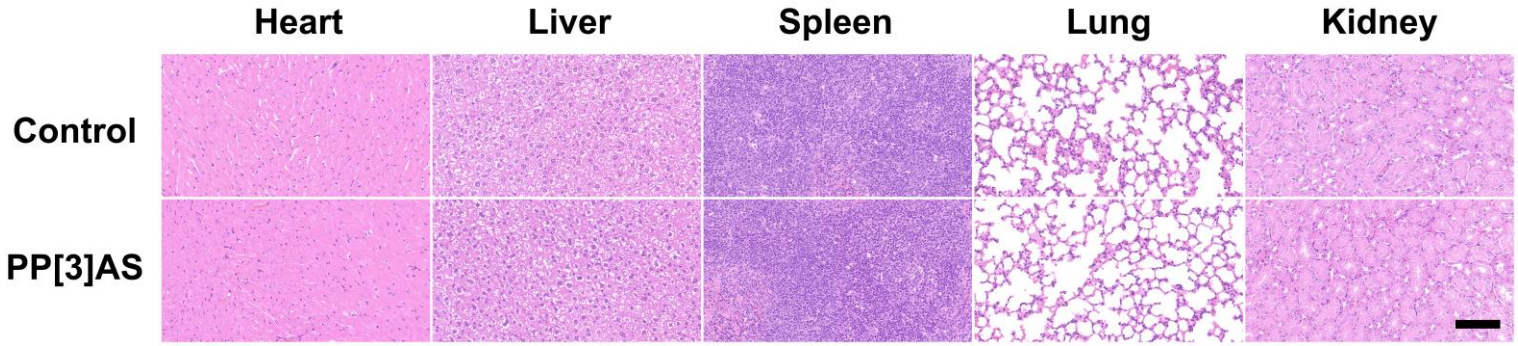

Fig. S28 H&E stains of the major organs from mice injected intraperitoneally with PP[3]AS compared with those injected with PBS (control group). The scale bar is 100 μm.

3.12 Comparison of anti-fibrillation potency.

Table S1 Anti-fibrillation capacities of PP[3]AS and several typical inhibitors.

Inhibitor	Temperature (°C)	Lag period (h)	Disaggregation level (%)	Ref.
.PP[3]AS	65	≥ 240	92.17	This work
CB[7]-PEG_{30k}	37	≥ 100	Incapacity	[10]
SC4AD	60	≥ 135	Incapacity	[11]
nChap-3[Zn]	37	Not mentioned	88	[12]
NCs-3	70	≥ 200	Incapacity	[13]
pep LVEALAL	25	≥ 80	Incapacity	[14]
Conjugate 4	65	≥ 30	Incapacity	[15]
Betaine	37	6.00 ± 0.08	Incapacity	[16]
Citrulline		9.12 ± 0.10	Incapacity	
Proline		9.48 ± 0.08	Incapacity	
Sorbitol		7.97 ± 0.08	Incapacity	
Rosmarinic acid	60	≥ 168	Incapacity	[17]

3.13 *In vivo* disintergrated insulin performance.

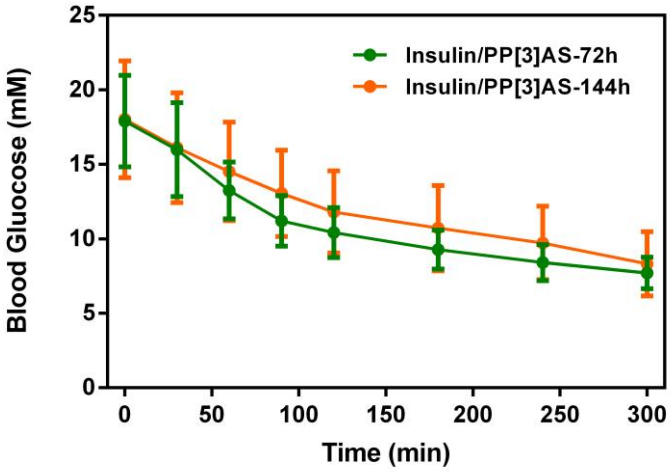

Fig. S29 Blood glucose concentration at predetermined intervals in STZ-induced diabetic mice after injection of disintergrated insulin which was co-incubated by PP[3]ASat 72 and 144 h after initiation of aggregation for 12 h (mean ± S.D., n = 6).

References

1 A. Henning, H. Bakirci, W. Nau, *Nat. Methods.*, 2007,**4**, 629-632.

2 G. Ghale, W. Nau, *Acc. Chem. Res.*, 2014, **47**, 2150−2159.

3 R. Dsouza, U. Pischel, W. Nau, *Chem. Rev.*, 2011, **111**, 7941-7980.

4 J. Collell, P. Ungerer, G. Galliero, M. Yiannourakou, F. Montel, M. Pujol, *Energy Fuels.*, 2014, **28**, 7457–7466.

5 T. Matthew, A. P. James, J. D. Robert, *J. Chem. Theory Comput.*, 2016, **12**, 1385-1392.

6 A. Bani-Yaseen, *J. Mol. Liq.* 2017, **227**, 280-290.

7 J. Chen, Y. Zhang, Z. Meng, L. Guo, X. Yuan, Y. Zhang, Y Chai, J. L. Sessler, Q. Meng, C. Li, *Chem. Sci.*, 2020, **11**, 6275-6282.

8 L. Gao, M. Li, S. Ehrmann, Z. Tu, R. Haag, *Angew. Chem. Int. Ed.*, 2019, **58**, 3645-3649.

9 S. Xian, Y. Xiang, D. Liu, B. Fan, K. Mitrová, R. C. Ollier, B. Su, M. A. Alloosh, J. Jiráček, M. Sturek, M. Alloosh, M. J. Webber, *Adv. Mater.*, 2024, **36**, 2308965.

10 M. J. Webber, E. A. Appel, B. Vinciguerra, A. B. Cortinas, L.S. Thapa, S. Jhunjhunwala, L. Isaacs, R. Langer, D. G. Anderson, *Proc. Natl. Acad. Sci.*, 2016, **113**, 14189–14194.

11 H. Zhao, X.Yang, Y. Pan, H. Tian, X. Hua, D. Guo, *Chin. Chem. Lett.*, 2020, **31**, 1873–1876.

12 H. Wang, A. Li, M. Yang, Y. Zhao, L. Shi, R. Ma, *Sci. China Chem.*, 2022, **65**, 353–362.

13 C. Li, X. Liu, Y. Zhang, J. Lv, F. Huang, G. Wu, Y. Liu, R. Ma, Y. An, and L. Shi, *Nano Lett.*, 2020, **20**, 1755–1765.

14 M. I. Ivanova, S. A. Sievers, M. R. Sawaya, et al., *Proc. Natl. Acad. Sci.*, 2009, **106**, 18990–18995.

15 N. K. Mishra, K. B. Joshi, S. Verma, *Mol. Pharm.*, 2013, **10**, 3903–3912.

16 S. Choudhary, N. Kishore, R.V. Hosur, *Sci. Rep.*, 2015, **5**, 17599.

17 Q. Zheng, N. D. Lazo, *J. Phys. Chem. B*, 2018, **122**, 2323−2331.